

Revisiting Skeleton-based Action Recognition

Haodong Duan¹ Yue Zhao² Kai Chen^{3,5} Dian Shao¹ Dahua Lin¹ Bo Dai⁴

¹The Chinese University of HongKong ²The University of Texas at Austin

³SenseTime Research ⁴S-Lab, Nanyang Technological University ⁵Shanghai AI Laboratory

Abstract

Human skeleton, as a compact representation of human action, has received increasing attention in recent years. Many skeleton-based action recognition methods adopt graph convolutional networks (GCN) to extract features on top of human skeletons. Despite the positive results shown in previous works, GCN-based methods are subject to limitations in robustness, interoperability, and scalability. In this work, we propose PoseC3D, a new approach to skeleton-based action recognition, which relies on a 3D heatmap stack instead of a graph sequence as the base representation of human skeletons. Compared to GCN-based methods, PoseC3D is more effective in learning spatiotemporal features, more robust against pose estimation noises, and generalizes better in cross-dataset settings. Also, PoseC3D can handle multiple-person scenarios without additional computation cost, and its features can be easily integrated with other modalities at early fusion stages, which provides a great design space to further boost the performance. On four challenging datasets, PoseC3D consistently obtains superior performance, when used alone on skeletons and in combination with the RGB modality.

1. Introduction

Action recognition is a central task in video understanding. Existing studies have explored various modalities for feature representation, such as RGB frames [36, 31, 3], optical flows [28], audio waves [37], and human skeletons [39]. Among these modalities, skeleton-based action recognition has received increasing attention in recent years due to its action-focusing nature and compactness. In practice, human skeletons in a video are mainly represented as a sequence of human joint coordinate lists, where the coordinates are extracted by pose estimation methods. Since only the pose information is included, skeleton sequences capture only the human action information, while being immune to contextual nuisances, such as background variation and lighting changes.

Among all the methods for skeleton-based action recog-

nition [8, 35, 34], graph convolutional networks (GCN) [39] have been one of the most popular approaches. Specifically, GCN regards every human joint at every timestep as a node, and neighboring nodes along the spatial and temporal dimensions are connected with edges. Graph convolution layers are then applied on the constructed graph to discover action patterns across space and time. Given its performance in standard benchmarks for skeleton-based action recognition, people tend to take GCN for granted when processing skeleton sequences.

While showing encouraging results in previous works, GCN-based methods are limited in the following aspects: 1) *Robustness*: While GCN directly handles coordinates of human joints, its recognition ability is significantly affected by the distribution shift of coordinates, which can often occur when applying a different pose estimator to acquire the coordinates. Therefore a small perturbation in coordinates often leads to completely different predictions [40]. 2) *Interoperability*: Previous works have shown that representations from different modalities, such as RGB, optical flows, and skeletons are complementary. Hence, an effective combination of such modalities can often result in a performance boost in action recognition. However, the graphical form of the skeleton representation makes it difficult to be fused with other modalities, especially in early or low-level stages, thus limiting the effectiveness of the combination. 3) *Scalability*: In addition, since GCN regards every human joint as a node, the complexity of GCN scales linearly with the number of persons, limiting its applicability to tasks that involve multiple persons, such as group activity recognition.

In this paper, we propose a novel framework **PoseC3D** that serves as a competitive alternative to GCN-based approaches. In particular, PoseC3D focuses on 2D skeletons considering the performance of pose estimators as shown in Figure 1, which will be reformulated as 2D heatmaps of skeleton joints rather than graphs. 2D heatmaps at different timesteps will be stacked along the temporal dimension to form a 3D heatmap volume. PoseC3D then adopts a 3D convolutional neural network on top of the 3D heatmap volume to recognize actions. The main differences between the proposed PoseC3D and GCN-based approaches are summa-

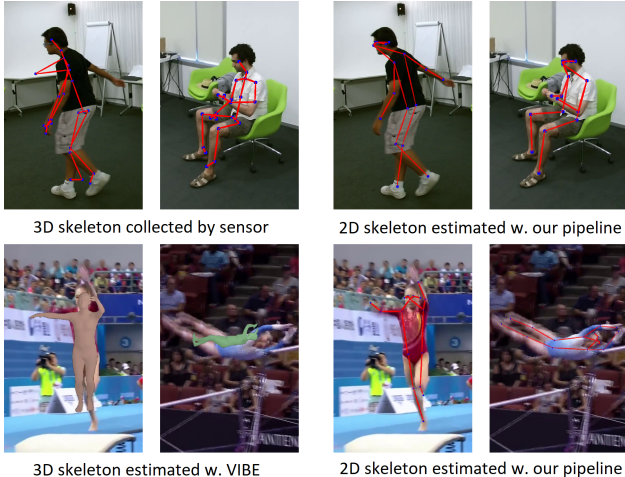


Figure 1: **3D skeleton is noisy.** We visualize 3D skeletons (collected by sensors or estimated with state-of-the-art estimators) and estimated 2D skeletons on two datasets: NTU-60 (line 1) and FineGYM (line 2). The 2D skeleton has superior quality.

	Previous Work	Ours
Input	2D / 3D Skeleton	2D Skeleton
Format	Coordinates	3D Heatmap Volumes
Architecture	GCN	3D-CNN

Table 1: **The differences between our pipeline and GCN.**

rized in Table 1.

The proposed PoseC3D well resolves the limitations of GCN-based approaches. The use of 3D heatmap volumes mitigates the sensitivity to pose estimation techniques: we empirically find that PoseC3D generalizes well across different scenarios and human skeletons obtained in different ways. Also, PoseC3D, which relies on heatmaps of the base representation, allows one to leverage the advances in convolutional network architectures and makes it much easier to integrate with other modalities in multi-stream convolutional networks. This opens up a great design space to further improve the recognition performance. Finally, the complexity of the 3D heatmap volume is invariant to the number of persons of interest. PoseC3D thus can handle different numbers of persons without increasing computational overhead. To verify the efficiency and effectiveness of PoseC3D, we conduct a comprehensive study across several datasets including FineGYM [26], NTURGB-D [21], Kinetics-400 [3] and Volleyball [13], where PoseC3D achieves the state-of-the-art performance compared to GCN-based approaches.

2. Related Work

3D-CNN for action recognition. 3D-CNN seems to be a natural approach for spatiotemporal feature learning

in videos, which has long been used in action recognition [14, 31]. Due to the large number of parameters, 3D-CNN requires huge amounts of videos to learn good representation. 3D-CNN has become the mainstream approach for action recognition since [3] proposed I3D and the large scale dataset Kinetics-400. From then on, many advanced 3D-CNN architectures [33, 11, 32, 10] were proposed by the action recognition community, which outperforms I3D both in recognition performance and efficiency. In this work, we first propose to use 3D-CNN for skeleton-based action recognition, rather than RGB or optical flow based one.

GCN for skeleton-based action recognition. Graph convolutional networks are widely adopted in skeleton-based action recognition, which model human skeleton sequences as spatial temporal graphs. ST-GCN [39] is a well-known baseline for GCN-based approaches, which combines spatial graph convolutions and interleaving temporal convolutions for spatiotemporal modeling. Upon the baseline, adjacency powering is used for multiscale modeling [22, 19] while self-attention mechanisms are utilized to improve the modeling capacity [27, 18]. Despite the great success of GCN in skeleton-based action recognition, it is also limited in robustness [40] and scalability. Besides, for GCN-based approaches, the feature fusion between skeletons and other modalities (RGB, *e.g.*) may need carefully design [6].

2D-CNN for skeleton-based action recognition. For skeleton-based action recognition, 2D-CNN-based approaches first model the skeleton sequence as a pseudo image based on some manually designed transformations. PoTion [5] aggregates heatmaps along the temporal dimension with color encodings to get the pose motion representation, while PA3D [38] does the aggregation with 1×1 convolutions. Although carefully designed, some information might still be lost during the aggregation, which can lead to inferior recognition performance¹. Other works [15, 1] directly convert the coordinates of a skeleton sequence to a pseudo image with some transformation, typically generate a 2D input of shape $K \times T$ ². Such kinds of input cannot exploit the locality nature of convolution networks, which makes these methods not as competitive as GCN on popular benchmarks [1]. Our work aggregates heatmaps by stacking them along the temporal dimension to form 3D heatmap volumes, no information is lost during this process. Besides, we use 3D-CNN instead of the 2D one, due to its good capability for spatiotemporal feature learning.

3. Framework

We propose **PoseC3D**, a 3D-CNN-based approach for skeleton-based action recognition, which can be a competitive alternative to GCN-based approaches that outperforms

¹During preliminary study, PoTion [5] achieves less than 85% Top-1 accuracy on FineGYM, while GCN or 3D-CNN achieve 90%+.

² K is the number of joints, T is the temporal length.

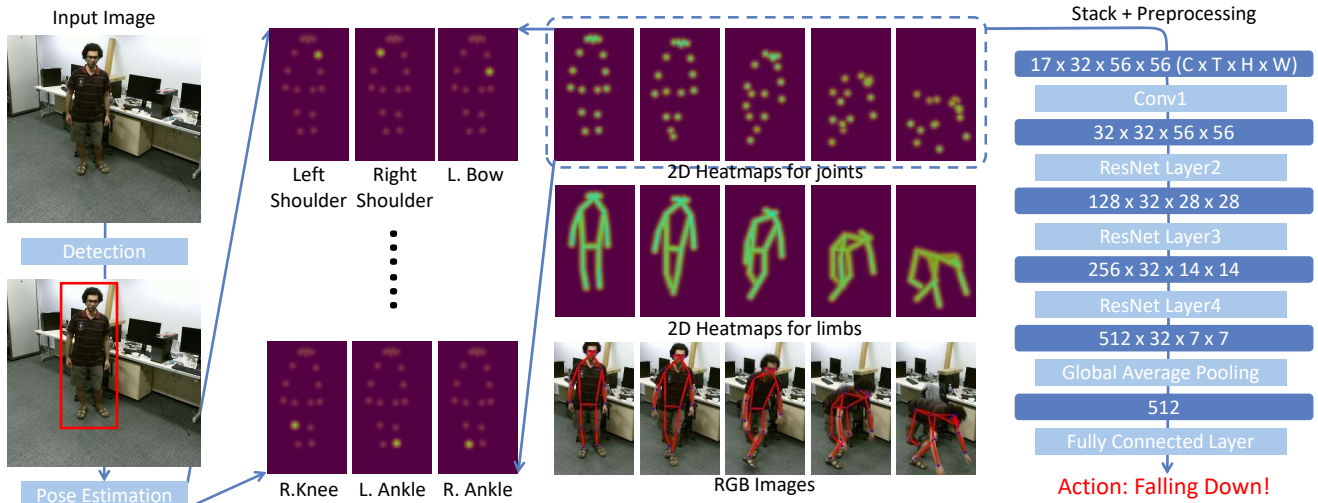


Figure 2: **Our Framework.** For each frame in a video, we first use a two-stage pose estimator (detection + pose estimation) for 2D human pose extraction. Then we stack heatmaps of joints or limbs along the temporal dimension and apply pre-processing to the generated 3D heatmap volumes. Finally, we use a 3D-CNN to classify the 3D heatmap volumes.

them in various settings and alleviates their limitations in robustness, interoperability, and scalability. An overview of PoseC3D is included in Figure 2, and details of PoseC3D will be covered in the following sections. We begin with a review of skeleton extraction, which is the basis of skeleton-based action recognition but is often overlooked in previous literature. We point out several aspects that should be considered when choosing a skeleton extractor and motivate the use of 2D skeletons in PoseC3D³. Subsequently, we introduce 3D Heatmap Volume that is the representation of a 2D skeleton sequence used in PoseC3D, and the structural designs of PoseC3D, including a variant that focuses on the modality of human skeletons as well as a variant that combines the modalities of human skeletons and RGB frames to demonstrate the interoperability of PoseC3D.

3.1. Good Practice for Pose Extraction

Being a critical pre-processing step for skeleton-based action recognition, pose or human skeleton extraction largely determines the final recognition accuracy. However, the importance of pose extraction is often overlooked in previous literature, which use poses estimated by sensors [25, 21] or existing pose estimators [39, 2] without considering their potential effects. We thus conduct a review on key aspects of pose extraction to find a good practice.

We mainly focus on 2D poses instead of 3D poses due to the quality gap between poses in demand and the ones estimated by existing 3D pose extractors, as shown in Figure 1. 2D pose estimators can be roughly divided into Top-

³PoseC3D can also work with 3D skeletons. An example is dividing a 3D skeleton (x, y, z) into three 2D skeletons respectively using (x, y) , (y, z) and (x, z) .

Down and BottomUp approaches, where the former starts by identifying individual instances using human detectors followed by extracting pose for each individual, and the latter acquires poses by grouping a set of identified key semantics into skeletons. In standard pose estimation benchmarks like COCO-keypoints [20], Top-Down approaches can outperform Bottom-Up ones by a large margin. When applied to action recognition, the advantage of Top-Down still preserves, in terms of both inference time and recognition precision. We thus choose Top-Down approaches, in particular HRNet [30] trained on COCO-keypoints as our pose extractor. We also study the effect of pose estimator quality on action recognition by instantiating the pose extractor with different backbones, and find the pose estimator quality is less important under the Top-Down framework. Finally, since Top-Down pose extractors estimate a number of bounding boxes for all instances in an image indiscriminately, the pose quality can be significantly improved if we can filter the boxes by our prior about the person of interest, e.g. knowing the ground-truth bounding box we interested.

3.2. From 2D Poses to 3D Heatmap Volumes

After 2D poses are extracted from frames of a video, to input them into PoseC3D, we reformulate them into a 3D heatmap volume. To begin with, we represent a 2D pose as a heatmap of size $K \times H \times W$, where K is the number of joints, H and W are respectively the height and width of the frame. We can directly use the heatmap produced by the TopDown pose estimator as the target heatmap, which should be zero-padded to match the size of the frame, since the corresponding bounding box is given. In cases we have only coordinates of skeleton joints, we can obtain a heatmap

\mathbf{H} by composing K gaussian maps centered at every joint:

$$\mathbf{H}_{kij} = \exp(-[(i - x_k)^2 + (j - y_k)^2]/(2 * \sigma^2)) * c_k, \quad (1)$$

where σ controls the variance of gaussian maps, and (x_k, y_k) and c_k are respectively the location and confidence score of k -th joint. We can also create a heatmap for limbs by stacking gaussian maps computed as:

$$v_{ij} = \exp(-d^2/(2 * \sigma^2)) * \min(c_i, c_j), \quad (2)$$

where v_{ij} is the value of a point on the gaussian map of the limb connecting i -th and j -th joints, and d is the minimal distance of that point to the limb connecting i -th and j -th joints. It's worth noting that although the above process assumes a single person in every frame, it can be easily extended to cases containing multiple persons, where we directly accumulate the k -th gaussian maps of all persons without enlarging the heatmap. Finally, a 3D heatmap volume is obtained by stacking all heatmaps along the temporal dimension, which thus has the size of $K \times T \times H \times W$.

In practice, we further apply two techniques to reduce the redundancy of 3D heatmap volumes. 1) *Subject Centered Cropping*. It is inefficient to make the heatmap as large as the frame, especially when all persons only occur in a small region. Therefore, in such cases we first find the smallest bounding box that encloses all the 2D poses across frames. Then we crop all frames according to the found box and resize them to a target size, so that the size of the 3D heatmap volume is reduced along the spatial dimensions. 2) *Uniform Sampling*. As PoseC3D is built upon 3D convolutional layers, the 3D heatmap volume can be reduced along the temporal dimension by sampling a subset of frames. However, researchers tend to sample frames in a short temporal window for 3D-CNNs, such as sampling frames in a 64-frame temporal window as in SlowFast [11]. While this sampling strategy may miss some global dynamics of the video, we propose to use a uniform sampling strategy [36] for 3D-CNNs instead. In particular, we sample n frames from the video by dividing the video into n segments of equal length and randomly selecting one frame from each segment. We find such a sampling strategy is especially beneficial for skeleton-based action recognition.

3.3. 3D-CNN for Skeleton-based Action Recognition

For skeleton-based action recognition, GCN has long been the mainstream backbone. In contrast, 3D-CNN, an effective network structure that are commonly used in RGB-based action recognition [3, 12, 11], is less explored in this direction. To demonstrate the power of 3D-CNN in capturing spatiotemporal dynamics of skeleton sequences, we design two networks based on 3D-CNNs, namely *Pose-SlowOnly* and *RGBPose-SlowFast*.

stage	RGB Pathway	Pose Pathway	output sizes $T \times S^2$
data layer	uniform $8, 1^2$	uniform $32, 4^2$	RGB: 8×224^2 Pose: 32×56^2
stem layer	conv $1 \times 7^2, 64$ stride $1, 2^2$ maxpool 1×3^2 stride $1, 2^2$	conv $1 \times 7^2, 32$ stride $1, 1^2$	RGB: 8×56^2 Pose: 32×56^2
res ₂	$\begin{bmatrix} 1 \times 1^2, 64 \\ 1 \times 3^2, 64 \\ 1 \times 1^2, 256 \end{bmatrix} \times 3$	N.A.	RGB: 8×56^2 Pose: 32×56^2
res ₃	$\begin{bmatrix} 1 \times 1^2, 128 \\ 1 \times 3^2, 128 \\ 1 \times 1^2, 512 \end{bmatrix} \times 4$	$\begin{bmatrix} 1 \times 1^2, 32 \\ 1 \times 3^2, 32 \\ 1 \times 1^2, 128 \end{bmatrix} \times 4$	RGB: 8×28^2 Pose: 32×28^2
res ₄	$\begin{bmatrix} 3 \times 1^2, 256 \\ 1 \times 3^2, 256 \\ 1 \times 1^2, 1024 \end{bmatrix} \times 6$	$\begin{bmatrix} 3 \times 1^2, 64 \\ 1 \times 3^2, 64 \\ 1 \times 1^2, 256 \end{bmatrix} \times 6$	RGB: 8×14^2 Pose: 32×14^2
res ₅	$\begin{bmatrix} 3 \times 1^2, 512 \\ 1 \times 3^2, 512 \\ 1 \times 1^2, 2048 \end{bmatrix} \times 3$	$\begin{bmatrix} 3 \times 1^2, 128 \\ 1 \times 3^2, 128 \\ 1 \times 1^2, 512 \end{bmatrix} \times 3$	RGB: 8×7^2 Pose: 32×7^2
	GAP, fc	GAP, fc	# classes

Table 2: **An instantiation of the RGBPose-SlowFast network.** The dimensions of kernels are denoted by $T \times S^2, C$ for temporal, spatial, channel sizes. Strides are denoted with T, S^2 for temporal and spatial strides. The Pose Pathway takes denser input, corresponds to the fast pathway in SlowFast. The backbone we use is ResNet50. GAP denotes global average pooling.

Pose-SlowOnly. The *Pose-SlowOnly* focuses on the modality of human skeletons, whose architecture is inspired by the slow pathway of SlowFast [11], given its promising performance in RGB-based action recognition. The detailed architecture of *Pose-SlowOnly* is included in Table 2 (*Pose Pathway*), which takes 3D heatmap volumes as input and differs from its original counterpart in several aspects: 1. *Pose-SlowOnly* has no downsampling operations in the stem layer, since its inputs are $4 \times$ smaller. 2. The res₂ layer for *Pose-SlowOnly* is removed for the 3D heatmap volumes are already mid-level features for action recognition, compared to low-level features like RGB frames. 3. The channel width is reduced to half of its original value which we empirically found is sufficient to model spatiotemporal dynamics of human skeleton sequences. In experiments, *Pose-SlowOnly* is shown to outperform the representative GCN counterpart across several benchmarks. More importantly, the interoperability between *Pose-SlowOnly* and popular networks for RGB-based action recognition makes it easy to involve human skeletons in multi-modality fusion.

RGBPose-SlowFast. We propose *RGBPose-SlowFast* for the early fusion of human skeletons and RGB frames, which is achieved due to the use of 3D-CNNs in skeleton-based action recognition. As shown in Table 2, *RGBPose-SlowFast* shares the same spirit with SlowFast [11]. It contains two pathways respectively for processing two modalities, where the RGB pathway is instantiated with a small frame rate and a large channel width since RGB frames are low-level

Pose	GYM	NTU-60
3D [Sensor]	N.A.	89.4
3D [VIBE]	87.0	N.A.
2D [HQ]	92.0	91.9
2D [LQ]	89.0	90.2

(a) **2D skeleton v.s. 3D skeleton.** HQ means high quality (HRNet), LQ means low quality (MobileNet).

	Mean-Top1
Detection	75.8
Tracking	85.3
GT	92.0

(c) **Performance of Pose extracted with different boxes.**

Model	COCO AP	NTU-60
HR-TD	0.746	93.6
HR-BU	0.654	93.0
Mobile-TD	0.646	92.0

(b) **Top-Down v.s. Bottom-Up approaches for pose estimation.** TD, BU are abbreviations for Top-Down and Bottom-Up.

	Mean-Top1
Coordinate [LQ]	90.7
Coordinate [HQ]	93.2
Heatmap [LQ]	92.7
Heatmap [HQ]	93.6

(d) **Coordinate v.s. Heatmap.** The meanings of LQ, HQ are the same as Table 3a.

Table 3: **Ablation study on Pose Extraction.**

features. On the contrary, the Pose pathway is instantiated with a large frame rate and a small channel width. Moreover, time-strided convolutions are used as the lateral connections between two pathways, so that semantics of different modalities can sufficiently interact. Some adjustments are made in *RGBPose-SlowFast* to better accommodate the characteristics of these two modalities. Specifically, res_2 of the Pose pathway is removed, and lateral connections are only added before res_3 and res_4 , where we use bidirectional lateral connections instead of unidirectional ones, since they are connecting two very different modalities, unlike the original *SlowFast*. Besides lateral connections, the predictions of two pathways are also combined in a late fusion manner, which leads to further improvements in our empirical study. Finally, we train *RGBPose-SlowFast* with two individual losses respectively for each pathway, as a single loss that jointly learns from two modalities leads to severe overfitting.

4. Experiments

4.1. Dataset Preparation

We use 4 datasets in our experiments: FineGYM [26], NTURGB-D [25, 21], Kinetics-400 [3, 39] and Volleyball [13]. Unless otherwise specified, for all datasets, we use the top-down approach for pose extraction: the detector is Faster-RCNN [23] with the ResNet50 backbone while the pose estimator is HRNet-w32 [30] pre-trained on COCO-keypoint [20].⁴ We report the **Mean-Top-1** accuracy for FineGYM and the **Top-1** accuracy for other 3 datasets.

FineGYM. FineGYM is a fine-grained action recognition dataset with 29K videos of 99 fine-grained gymnastic ac-

tion classes. During pose extraction, we compare three different kinds of person bounding boxes: 1. Person bounding boxes predicted by the detector (**Detection**); 2. GT bounding boxes for the athlete in the 1st frame, tracking boxes for the rest frames (**Tracking**). 3. GT bounding boxes for the athlete in all frames (**GT**). In experiments, we use human pose extracted with the 3_{rd} kind of bounding boxes unless otherwise noted.

NTURGB-D. NTURGB-D is a large-scale human action recognition dataset collected in the lab. It has two versions, named NTU-60 and NTU-120 (a superset of NTU-60): NTU-60 contains 57K videos of 60 human actions, while NTU-120 contains 114K videos of 120 human actions. The datasets are split in 3 ways: Cross-subject (**X-Sub**), Cross-view (**X-View**, for NTU-60), Cross-setup (**X-Set**, for NTU-120), for which action subjects, camera views, camera setups are different in training and validation. The 2D/3D keypoints collected by sensors are available for this dataset. Unless otherwise specified, we conduct experiments on the **X-sub** splits for NTU-60 and NTU-120.

Kinetics-400. Kinetics-400 is a large-scale action recognition dataset with 306K videos of 400 actions. The 2D keypoints [39] extracted with OpenPose [2] are available and widely used in previous literature. For Kinetics, experiments are conducted with both the old [39] and the newly extracted 2D pose annotations.

Volleyball. Volleyball is a group activity recognition dataset with 4830 videos of 8 group activity classes. Each frame in a video contains approximately 12 persons while only the center frame is annotated with GT person boxes. We use tracking boxes from [24] for pose extraction.

4.2. Pose Extraction

In this section, we discuss different alternatives which can be adopted in pose extraction to validate our choice. The input size for all 3D-CNN experiments is $T \times H \times W = 48 \times 56 \times 56$.

2D v.s. 3D Skeletons. We first compare the recognition performance of using 2D and 3D skeletons for action recognition. The 3D skeletons are either collected by sensors (NTU-60) or estimated with the state-of-the-art 3D pose estimator [16] (FineGYM). For a fair comparison, we use MS-G3D [22] (the current state-of-the-art GCN for skeleton-based action recognition) with the same configuration and training schedule for both 2D and 3D keypoints and list the results in Table 3a. The estimated 2D keypoints (even low-quality ones) consistently outperform 3D keypoints (sensor collected or estimated) in action recognition.

Bottom-Up v.s. Top-Down. To compare the pose estimation quality of bottom-up and top-down approaches, we instantiate the two approaches with the same architecture HRNet-w32 (HR-TD & HR-BU). Besides, we also instantiate the top-down approach with MobileNet-v2 backbone

⁴We will release all the 2D pose annotations used in our experiments.

(Mobile-TD) for comparison, which has similar performance to HR-BU on COCO-val. We use extracted heatmap volumes to train a *Pose-SlowOnly* on NTU-60. Table 3b shows that the performance of HR-BU on COCO-val is much worse than HR-TD and close to Mobile-TD. However, the Top-1 accuracy of HR-BU is much higher than Mobile-TD and close to HR-TD. Although the potential of Bottom-Up should not be neglected, considering the better performance and faster inference speed (Top-Down runs faster when there aren't many persons in a frame), we use Top-Down for pose extraction in this work.

Interested Person v.s. All Persons. There may exist many people in a video but not all of them are related to the action to be recognized. For example, in FineGYM, only the pose of the athlete is useful, while other persons like the audience or referee are unrelated. We compare using 3 kinds of person bounding boxes for pose extraction: **Detection**, **Tracking** and **GT** (with increasing prior about the athlete). In Table 3c, we see that the prior of the interested person is extremely important: even a weak prior (1 GT box per video) can improve the performance by a large margin.

Coordinates v.s. Heatmaps. Storing 3D heatmap volumes may take extraordinarily large amounts of disk space. To be more efficient, we can store the 2D pose as coordinates (x, y, score), and restore them to 3D heatmap volumes following the methods we introduced in Sec. 3.2. We conduct experiments on FineGYM to explore how much information is lost during the heatmap→coordinate compression. In Table 3d, we see that for low-quality (LQ) pose estimators, it leads to a 2% drop in Mean-Top1. For high-quality (HQ) ones, the degradation is more moderate (only a 0.4% Mean-Top1 drop). Thus we choose to store coordinates instead of 3D heatmap volumes.

4.3. Preprocessing of 3D Heatmap Volumes

Subjects-Centered Cropping. Since the sizes and locations of persons can vary a lot in the dataset, focusing on the action subjects is the key to reserve as much information as possible with a relatively small $H \times W$ budget. To validate this, we conduct a pair of experiments on NTU-60 with input size $32 \times 56 \times 56$, with or without subjects-centered cropping. It turns out that subjects-centered cropping is a useful step in data preprocessing, which improves the Top1 accuracy by 1.0%, from 92.2% to 93.2%.

Uniform Sampling. The input sampled from a small temporal window may not capture the full dynamic of the human action. To validate this, we conduct experiments on FineGYM and NTU-60: for fixed stride sampling which samples from a fixed temporal window, we try to sample 32 frames with the temporal stride 2, 3, 4; for uniform sampling, we sample 32 frames uniformly from the entire clip. From Figure 3, we see that uniform sampling consistently outperforms sampling with fixed temporal strides.

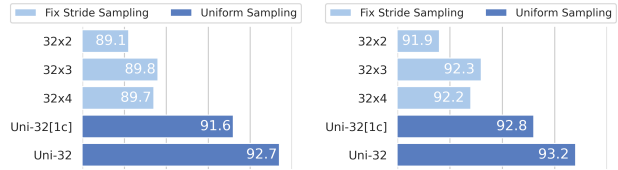


Figure 3: **Uniform Sampling outperforms Fix Stride Sampling.** All results are for 10-clip testing, except Uni-32[1c], which uses 1-clip testing. Left: FineGYM, Right: NTU-60.

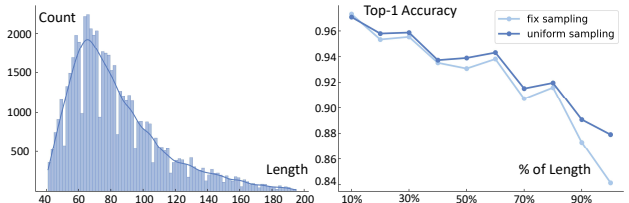


Figure 4: **Uniform Sampling helps in modeling longer videos.** Left: The length distribution of NTU60 (X-Sub) validation videos. Right: Uniform Sampling helps improve the recognition accuracy of videos in the validation set, mainly for longer videos.

With uniform sampling, 1-clip testing can even achieve better results than fixed stride sampling with 10-clip testing. Note that the video length can vary a lot in NTU-60 and FineGYM. In a more detailed analysis, we find that uniform sampling mainly improves the recognition performance for longer videos in the dataset (Figure 4). Besides, uniform sampling also outperforms fixed stride sampling on RGB-based recognition on these two datasets⁵.

Pseudo Heatmaps: Joints or Limbs? Based on the coordinates we saved, we can generate pseudo heatmaps for joints and limbs. In general, we find that pseudo heatmaps for joints are better inputs for a 3D-CNN, while pseudo heatmaps for limbs lead to comparable or inferior performance. Ensembling two models trained respectively on the limb and joint heatmaps can lead to further improvement.

4.4. Comparison with GCN

In this section, we compare our 3D-CNN-based approach with GCN ones in multiple dimensions including performance, robustness and scalability. The GCN we compared to is MS-G3D [22], the current state-of-the-art work in skeleton-based action recognition, trained with the hyperparameters provided in the original paper.

4.4.1 Performance.

In performance comparison between 3D-CNN and GCN, we adopt the input shape $48 \times 56 \times 56$ for 3D-CNN, which

⁵Please refer to the supplementary for details and discussions.

Dataset	GCN			3D-CNN			
	Acc	Params	FLOPs	1-clip	10-clip	Params	FLOPs
FineGYM	92.0	2.8M	24.7G	92.4	93.2	2.0M	15.9G
NTU-60	91.9	2.8M	16.7G	93.1	93.7		
NTU-120	84.8	2.8M	16.7G	85.1	86.0		
Kinetics-400	44.9	2.8M	17.5G	44.8	46.0		

Table 4: **3D-CNN vs. GCN.** We compare the performance of 3D-CNN and GCN on several datasets. For 3D-CNN, we report the results of 1/10-clip testing. We don’t count parameters and FLOPs of the FC layer, since it depends on the number of classes.

p	0	1/8	1/4	1/2	1
GCN	92.0	91.0	90.2	86.5	77.7
GCN (robust train)	90.9	91.0	91.0	91.0	90.6
3D-CNN	92.4	92.4	92.3	92.1	91.5

Table 5: **Recognition performance w. different dropping KP probabilities.** 3D-CNN is more robust to input perturbations. (1-clip testing is used for 3D-CNN)

is a light-weighted configuration. From Table 4, we see that under such configuration, our PoseC3D is even lighter than the GCN counterpart, both in the number of parameters and FLOPs. Although being light-weighted, PoseC3D still achieves competitive performance across different datasets. The 1-clip testing result is better than or comparable with a state-of-the-art GCN while requiring much less computation. When applying 10-clip testing, PoseC3D consistently outperforms the state-of-the-art GCN. Note that only PoseC3D can take advantage of multi-view testing, since it subsamples from the entire heatmap volumes to form each input. Besides, PoseC3D uses the same architecture and hyperparameters for different datasets and achieves competitive performance, while GCN tunes architectures and hyperparameters for different datasets [22].

4.4.2 Robustness & Generalization.

Robustness. To test the robustness of both models, we can drop a proportion of keypoints in the input and see how such perturbation will affect the final accuracy. Since limb keypoints⁶ are more important for gymnastics than torso or face keypoints, we test both models by randomly dropping 1 limb keypoint in each frame with probability p . In Table 5, we see that 3D-CNN is extremely robust to input perturbations: dropping 1 limb keypoint per frame only leads to a moderate drop (less than 1%) in Mean-Top1, while the drop for GCN is 14.3%. Someone would argue that we can train GCN with the noisy input, similar to the dropout operation [29]. However, even under this setting, the Mean-Top1 accuracy of GCN also drops by 1.4% for the case $p = 1$. Besides, with robust training, there will be an additional 1.1% drop for the case $p = 0$. The experiment results show that 3D-CNN significantly outperforms GCN in terms of robustness for pose recognition.

Generalization. To study the generalization of 3D-CNN

⁶There are 8 limb keypoints: bow, wrist, knee, ankle (left/right).

GCN Test/Train	LQ	HQ	3D-CNN Test/Train	LQ	HQ
	LQ	89.0		79.3	LQ
HQ	87.9	92.0	HQ	91.6	93.2

1. Train/Test w. Pose from different estimators

GCN Test/Train	Track	GT	3D-CNN Test/Train	Track	GT
	Track	82.9		78.5	Track
GT	89.1	92.0	GT	90.6	93.2

2. Train/Test w. Pose extracted with different boxes

Figure 5: **Train & Test w. Pose Annotations extracted by different approaches.** 3D-CNN shows great generalization capability in the cross-PoseAnno setting (the larger the anti-diagonal values, the better).

and GCN, we design a cross-annotation setting for training & testing on FineGYM. Specifically, we use pose extracted by HRNet for training, and pose extracted by MobileNet for testing. From Figure 5, we first find that for 3D-CNN, the performance drop when using the pose of low quality for training & testing is more moderate than GCN. Besides, when using poses extracted by different approaches (**GT**, **Tracking**) for training and testing respectively, the performance drop of 3D-CNN is much smaller than GCN. The experiment results show that 3D-CNN can generalize better than GCN.

4.4.3 Scalability.

The computation of GCN scales linearly with the increasing number of persons in the video, which makes it less efficient for group activity recognition. An experiment on the Volleyball dataset [13] is used to prove that. The dataset contains at most 13 persons in a frame, while the temporal length we use is 20, so the input shape of GCN is $13 \times 20 \times 17 \times 3$. Under such configuration, the number of parameters and FLOPs for GCN is 2.8M and 7.2G respectively. For 3D-CNN, we sample 12 frames out of 20 to form a heatmap volume of shape $17 \times 12 \times 56 \times 56$ and use 16 as the base channel width for the 3D-CNN. Under such configuration, 3D-CNN only takes 0.52M parameters and 1.6 GFLOPs (with 1-clip testing). Despite the much smaller amounts of parameters and FLOPs, 3D-CNN achieves 91.3% Top-1 accuracy on Volleyball-validation, which is 2.1% higher than the GCN-based approach.

4.5. RGBPose-SlowFast

The 3D-CNN architecture of PoseC3D makes it more flexible to fuse pose with other modalities via some early fusion strategies. For example, in *RGBPose-SlowFast*, lateral connections between *RGB*-pathway and *Pose*-pathway are exploited for cross-modality feature fusion in the early

	LateFusion	RGB→Pose	Pose→RGB	Bi-Directional
1-clip	92.6	93.0	93.4	93.6
10-clip	93.4	93.7	93.8	94.1

Table 6: **The design of *RGBPose-SlowFast*.** Bi-directional lateral connections outperform uni-directional ones in the early stage feature fusion. Mean-Top1 on FineGYM is reported.

	RGB	Pose	LateFusion	<i>RGBPose-SlowFast</i>
FineGYM	87.2 / 88.5	91.0 / 92.0	92.6 / 93.4	93.6 / 94.1
NTU-60	94.1 / 94.9	92.8 / 93.2	95.5 / 96.0	96.2 / 96.5

Table 7: **The universality of *RGBPose-SlowFast*.** The **early+late** fusion strategy works both on RGB-dominant dataset NTU-60 and Pose-dominant dataset FineGYM.

stage. In practice, we first train two models, *i.e.* RGB-Only and Pose-Only models separately and use them to initialize the *RGBPose-SlowFast*. We continue to finetune the network for several epochs to train the lateral connections. The final prediction is achieved by late fusing the prediction logits from both pathways. In a word, *RGBPose-SlowFast* can achieve better fusing results with **early+late** fusion.

Our experiments are based on *RGBPose-SlowFast* instantiated as Table 2. We first compare uni-directional lateral connections and bi-directional lateral connections in Table 6. The result shows that bi-directional feature fusion is better than uni-directional ones for RGB and Pose. With bi-directional feature fusion in the early stage, the **early+late** fusion with 1-clip testing can outperform the **late** fusion with 10-clip testing. Besides, *RGBPose-SlowFast* also works in situations when the importance of two modalities are different. In FineGYM, Pose modality is more important than RGB, while in NTU-60, RGB modality is more important than Pose, yet we observe performance improvement by **early+late** fusion on both of them in Table 7.

4.6. Comparison with state-of-the-arts

Skeleton-based Action Recognition. PoseC3D achieves competitive results on multiple datasets. In Table 8, we compare the performance of PoseC3D with previous state-of-the-arts. The architecture of PoseC3D is demonstrated in Table 2 (*Pose-Pathway*), with the input size $48 \times 56 \times 56$. We store the extracted pose as coordinates and use them to generate pseudo heatmaps for joints and limbs. We report the 10-clip testing performance of the ensemble of the joint model and limb model. As far as we know, no work aims at skeleton-based action recognition on FineGYM before (except the baseline in [26]), while our work first improves the performance to a decent level. For NTURGB-D, previous methods focus on GCN-based recognition with 3D-skeleton input, yet we prove that high-quality 2D-skeleton with 3D-CNN can yield comparable or

Dataset	Previous state-of-the-art	Ours
FineGYM-99	25.2 [26] (2D-Ske)	94.3
NTU60 (X-Sub)	91.5 [22] (3D-Ske)	94.1
NTU60 (X-View)	96.6 [4] (3D-Ske)	97.1
NTU120 (X-Sub)	86.9 [22] (3D-Ske)	86.9
NTU120 (X-Set)	88.4 [22] (3D-Ske)	90.3
Kinetics (OpenPose [2])	38.0 [22] (2D-Ske)	38.0
Kinetics (Ours)	44.9 [22] (2D-Ske)	47.7

Table 8: **PoseC3D is better or comparable to previous state-of-the-arts.** With estimated high-quality 2D skeleton and the great capacity of 3D-CNN to learn spatio-temporal features, PoseC3D achieves competitive performance across several benchmarks.

Dataset	Previous state-of-the-art	Ours
FineGYM-99	87.7 [17]	95.6
NTU60 (X-Sub)	95.7 [7]	97.0
NTU120 (X-Sub)	94.5 [7]	95.3

Table 9: ***RGBPose-SlowFast* achieves the state-of-the-art performance across various benchmarks.**

better performance. On Kinetics, when both using the low-quality 2D-skeleton, our method is comparable with the previous state-of-the-art. When both using the high-quality one, our method outperforms previous methods by a significant margin.

RGB + skeleton-based Action Recognition. Being a powerful representation itself, skeletons are also complementary to other modalities, like RGB appearance. We apply the proposed *RGBPose-SlowFast* to various datasets. We use ResNet50 as the backbone, 16, 48 as the temporal length for *RGB-Pathway* and *Pose-Pathway*. Table 9 shows that our **early+late** fusion strategy achieves excellent performance across various benchmarks. Due to the large size of Kinetics-400, we fuse the prediction of PoseC3D with the RGB based prediction by irCSN-152+OmniSource [9] instead. The late fusion between skeleton and RGB further improves the Top-1 accuracy by 0.3%, reaches a new state-of-the-arts on Kinetics-400 (**83.9%**).

5. Conclusion

In this work, we propose **PoseC3D**: a 3D-CNN-based approach for skeleton-based action recognition, which takes 3D heatmap volumes as input. PoseC3D resolves the limitations of GCN-based approaches in *robustness*, *interoperability* and *scalability*. With light-weighted 3D-ConvNets and compact 3D heatmap volumes as input, PoseC3D outperforms GCN-based approaches in both accuracy and efficiency. Based on PoseC3D, we achieve the state-of-the-art on both skeleton-based and RGB+skeleton-based action recognition across various benchmarks.

References

- [1] Carlos Caetano, Jessica Sena, François Brémond, Jefferson A Dos Santos, and William Robson Schwartz. Skelemotion: A new representation of skeleton joint sequences based on motion information for 3d action recognition. In *2019 16th IEEE International Conference on Advanced Video and Signal Based Surveillance (AVSS)*, pages 1–8. IEEE, 2019. 2
- [2] Z. Cao, G. Hidalgo Martinez, T. Simon, S. Wei, and Y. A. Sheikh. Openpose: Realtime multi-person 2d pose estimation using part affinity fields. *IEEE Transactions on Pattern Analysis and Machine Intelligence*, 2019. 3, 5, 8
- [3] Joao Carreira and Andrew Zisserman. Quo vadis, action recognition? a new model and the kinetics dataset. In *proceedings of the IEEE Conference on Computer Vision and Pattern Recognition*, pages 6299–6308, 2017. 1, 2, 4, 5
- [4] Ke Cheng, Yifan Zhang, Congqi Cao, Lei Shi, Jian Cheng, and Hanqing Lu. Decoupling gcn with dropgraph module for skeleton-based action recognition. 8
- [5] Vasileios Choutas, Philippe Weinzaepfel, Jérôme Revaud, and Cordelia Schmid. Potion: Pose motion representation for action recognition. In *Proceedings of the IEEE conference on computer vision and pattern recognition*, pages 7024–7033, 2018. 2
- [6] Srijan Das, Saurav Sharma, Rui Dai, Francois Bremond, and Monique Thonnat. Vpn: Learning video-pose embedding for activities of daily living. In *European Conference on Computer Vision*, pages 72–90. Springer, 2020. 2
- [7] Mahdi Davoodikakhki and KangKang Yin. Hierarchical action classification with network pruning. In *International Symposium on Visual Computing*, pages 291–305. Springer, 2020. 8
- [8] Yong Du, Wei Wang, and Liang Wang. Hierarchical recurrent neural network for skeleton based action recognition. In *Proceedings of the IEEE conference on computer vision and pattern recognition*, pages 1110–1118, 2015. 1
- [9] Haodong Duan, Yue Zhao, Yuanjun Xiong, Wentao Liu, and Dahua Lin. Omni-sourced webly-supervised learning for video recognition. *arXiv preprint arXiv:2003.13042*, 2020. 8
- [10] Christoph Feichtenhofer. X3d: Expanding architectures for efficient video recognition. In *Proceedings of the IEEE/CVF Conference on Computer Vision and Pattern Recognition*, pages 203–213, 2020. 2
- [11] Christoph Feichtenhofer, Haoqi Fan, Jitendra Malik, and Kaiming He. Slowfast networks for video recognition. In *Proceedings of the IEEE/CVF International Conference on Computer Vision*, pages 6202–6211, 2019. 2, 4
- [12] Kensho Hara, Hirokatsu Kataoka, and Yutaka Satoh. Can spatiotemporal 3d cnns retrace the history of 2d cnns and imagenet? In *Proceedings of the IEEE conference on Computer Vision and Pattern Recognition*, pages 6546–6555, 2018. 4
- [13] Mostafa S Ibrahim, Srikanth Muralidharan, Zhiwei Deng, Arash Vahdat, and Greg Mori. A hierarchical deep temporal model for group activity recognition. In *Proceedings of the IEEE Conference on Computer Vision and Pattern Recognition*, pages 1971–1980, 2016. 2, 5, 7
- [14] Shuiwang Ji, Wei Xu, Ming Yang, and Kai Yu. 3d convolutional neural networks for human action recognition. *IEEE transactions on pattern analysis and machine intelligence*, 35(1):221–231, 2012. 2
- [15] Qihong Ke, Mohammed Bennamoun, Senjian An, Ferdous Sohel, and Farid Boussaid. A new representation of skeleton sequences for 3d action recognition. In *Proceedings of the IEEE conference on computer vision and pattern recognition*, pages 3288–3297, 2017. 2
- [16] Muhammed Kocabas, Nikos Athanasiou, and Michael J Black. Vibe: Video inference for human body pose and shape estimation. In *Proceedings of the IEEE/CVF Conference on Computer Vision and Pattern Recognition*, pages 5253–5263, 2020. 5
- [17] Heeseung Kwon, Manjin Kim, Suha Kwak, and Minsu Cho. Learning self-similarity in space and time as generalized motion for action recognition. *arXiv preprint arXiv:2102.07092*, 2021. 8
- [18] Bin Li, Xi Li, Zhongfei Zhang, and Fei Wu. Spatio-temporal graph routing for skeleton-based action recognition. In *Proceedings of the AAAI Conference on Artificial Intelligence*, volume 33, pages 8561–8568, 2019. 2
- [19] Maosen Li, Siheng Chen, Xu Chen, Ya Zhang, Yanfeng Wang, and Qi Tian. Actional-structural graph convolutional networks for skeleton-based action recognition. In *Proceedings of the IEEE/CVF Conference on Computer Vision and Pattern Recognition*, pages 3595–3603, 2019. 2
- [20] Tsung-Yi Lin, Michael Maire, Serge Belongie, James Hays, Pietro Perona, Deva Ramanan, Piotr Dollár, and C Lawrence Zitnick. Microsoft coco: Common objects in context. In *European conference on computer vision*, pages 740–755. Springer, 2014. 3, 5
- [21] Jun Liu, Amir Shahroudy, Mauricio Perez, Gang Wang, Ling-Yu Duan, and Alex C. Kot. Ntu rgb+d 120: A large-scale benchmark for 3d human activity understanding. *IEEE Transactions on Pattern Analysis and Machine Intelligence*, 2019. 2, 3, 5
- [22] Ziyu Liu, Hongwen Zhang, Zhenghao Chen, Zhiyong Wang, and Wanli Ouyang. Disentangling and unifying graph convolutions for skeleton-based action recognition. In *Proceedings of the IEEE/CVF Conference on Computer Vision and Pattern Recognition*, pages 143–152, 2020. 2, 5, 6, 7, 8
- [23] Shaoqing Ren, Kaiming He, Ross Girshick, and Jian Sun. Faster r-cnn: Towards real-time object detection with region proposal networks. *arXiv preprint arXiv:1506.01497*, 2015. 5
- [24] Kohei Sendo and Norimichi Ukita. Heatmapping of people involved in group activities. In *16th International Conference on Machine Vision Applications (MVA)*, 2019. 5
- [25] Amir Shahroudy, Jun Liu, Tian-Tsong Ng, and Gang Wang. Ntu rgb+d: A large scale dataset for 3d human activity analysis. In *IEEE Conference on Computer Vision and Pattern Recognition*, June 2016. 3, 5
- [26] Dian Shao, Yue Zhao, Bo Dai, and Dahua Lin. Finegym: A hierarchical video dataset for fine-grained action understanding. In *Proceedings of the IEEE/CVF Conference on Computer Vision and Pattern Recognition*, pages 2616–2625, 2020. 2, 5, 8

- [27] Lei Shi, Yifan Zhang, Jian Cheng, and Hanqing Lu. Two-stream adaptive graph convolutional networks for skeleton-based action recognition. In *Proceedings of the IEEE/CVF Conference on Computer Vision and Pattern Recognition*, pages 12026–12035, 2019. [2](#)
- [28] Karen Simonyan and Andrew Zisserman. Two-stream convolutional networks for action recognition in videos. *arXiv preprint arXiv:1406.2199*, 2014. [1](#)
- [29] Nitish Srivastava, Geoffrey Hinton, Alex Krizhevsky, Ilya Sutskever, and Ruslan Salakhutdinov. Dropout: a simple way to prevent neural networks from overfitting. *The journal of machine learning research*, 15(1):1929–1958, 2014. [7](#)
- [30] Ke Sun, Bin Xiao, Dong Liu, and Jingdong Wang. Deep high-resolution representation learning for human pose estimation. In *Proceedings of the IEEE/CVF Conference on Computer Vision and Pattern Recognition*, pages 5693–5703, 2019. [3](#), [5](#)
- [31] Du Tran, Lubomir Bourdev, Rob Fergus, Lorenzo Torresani, and Manohar Paluri. Learning spatiotemporal features with 3d convolutional networks. In *Proceedings of the IEEE international conference on computer vision*, pages 4489–4497, 2015. [1](#), [2](#)
- [32] Du Tran, Heng Wang, Lorenzo Torresani, and Matt Feiszli. Video classification with channel-separated convolutional networks. In *Proceedings of the IEEE/CVF International Conference on Computer Vision*, pages 5552–5561, 2019. [2](#)
- [33] Du Tran, Heng Wang, Lorenzo Torresani, Jamie Ray, Yann LeCun, and Manohar Paluri. A closer look at spatiotemporal convolutions for action recognition. In *Proceedings of the IEEE conference on Computer Vision and Pattern Recognition*, pages 6450–6459, 2018. [2](#)
- [34] Raviteja Vemulapalli, Felipe Arrate, and Rama Chellappa. Human action recognition by representing 3d skeletons as points in a lie group. In *Proceedings of the IEEE conference on computer vision and pattern recognition*, pages 588–595, 2014. [1](#)
- [35] Jiang Wang, Zicheng Liu, Ying Wu, and Junsong Yuan. Mining actionlet ensemble for action recognition with depth cameras. In *2012 IEEE Conference on Computer Vision and Pattern Recognition*, pages 1290–1297. IEEE, 2012. [1](#)
- [36] Limin Wang, Yuanjun Xiong, Zhe Wang, Yu Qiao, Dahua Lin, Xiaoou Tang, and Luc Van Gool. Temporal segment networks: Towards good practices for deep action recognition. In *European conference on computer vision*, pages 20–36. Springer, 2016. [1](#), [4](#)
- [37] Fanyi Xiao, Yong Jae Lee, Kristen Grauman, Jitendra Malik, and Christoph Feichtenhofer. Audiovisual slowfast networks for video recognition. *arXiv preprint arXiv:2001.08740*, 2020. [1](#)
- [38] An Yan, Yali Wang, Zhifeng Li, and Yu Qiao. Pa3d: Pose-action 3d machine for video recognition. In *Proceedings of the IEEE/CVF Conference on Computer Vision and Pattern Recognition*, pages 7922–7931, 2019. [2](#)
- [39] Sijie Yan, Yuanjun Xiong, and Dahua Lin. Spatial temporal graph convolutional networks for skeleton-based action recognition. In *Proceedings of the AAAI conference on artificial intelligence*, volume 32, 2018. [1](#), [2](#), [3](#), [5](#)
- [40] Dingyuan Zhu, Ziwei Zhang, Peng Cui, and Wenwu Zhu. Robust graph convolutional networks against adversarial attacks. In *Proceedings of the 25th ACM SIGKDD International Conference on Knowledge Discovery & Data Mining*, pages 1399–1407, 2019. [1](#), [2](#)